HHS Public Access

Author manuscript

Cancer Lett. Author manuscript; available in PMC 2023 January 28.

Published in final edited form as:

Cancer Lett. 2022 January 28; 525: 170–178. doi:10.1016/j.canlet.2021.10.042.

Enzalutamide-induced and PTH1R-mediated TGFBR2 degradation in osteoblasts confers resistance in prostate cancer bone metastases

Shang Su[1,2,#], **Jingchen Cao**[1,#], **Xiangqi Meng**[1,3,#], **Ruihua Liu**[1,2,4], **Alexandra Vander Ark**[1], **Erica Woodford**[1], **Reian Zhang**[1,5], **Isabelle Stiver**[1,5], **Xiaotun Zhang**[6], **Zachary B. Madaj**[7], **Megan J. Bowman**[1,8], **Yingying Wu**[9,10], **H. Eric Xu**[1,11], **Bin Chen**[9], **Haiquan Yu**[4], **Xiaohong Li**[1,2,*]

[1]Center for Cancer and Cell Biology, Van Andel Institute, Grand Rapids, MI, 49503;

[2]Current address: Department of Cancer Biology, the University of Toledo, Toledo, OH, 43614;

[3]Current address: The Sixth Affiliated Hospital of Sun Yat-sen University, Guangzhou, 510655, China;

[4]Inner Mongolia University, Hohhot, 010021, China;

[5]University of Michigan, Ann Arbor, MI, 48109;

[6]Anatomic/Clinical Pathology, Mayo Clinic, Rochester, MN, 55905;

[7]Bioinformatics & Biostatistics Core, Van Andel Institute, Grand Rapids, MI, 49503;

[8]Current address: Ball Horticultural Company, West Chicago, IL, 60185;

[9]Department of Pediatrics and Human Development, College of Human Medicine, Michigan State University, Grand Rapids, MI, 49503;

[10]Current address: Center of Mathematical Sciences and Applications, Harvard University, Cambridge, MA 02138;

[11]Current address: Shanghai Institute of Materia Medica, Chinese Academy of Sciences, Shanghai, 201203, China

[*]**Corresponding author**: Xiaohong Li, the University of Toledo, 3000 Transverse Drive, Toledo, OH 43614. Phone: +1-419-383-3982; xiaohong.li@utoledo.edu.

Author contributions

XL conceived and directed the project. XL, SS, and JC wrote the manuscript. XL, SS, JC, and XM designed, performed the experiments, and analyzed the data with help from RL, AVA, EW, RZ, and IS. XZ scored the cell-specific TGFBR2 expressions in tissue microarray. ZM and YW performed the statistical analyses. MB conducted the MetaCore analysis. HEX, BC, and HY provided resources. All authors have read and agreed to the published version of the manuscript.

[#]These authors contributed equally.

Conflict of Interest Disclosure: The authors declare no potential conflicts of interest.

Declaration of interests

The authors declare that they have no known competing financial interests or personal relationships that could have appeared to influence the work reported in this paper.

Abstract

Enzalutamide resistance has been observed in approximately 50% of patients with prostate cancer (PCa) bone metastases. Therefore, there is an urgent need to investigate the mechanisms and develop strategies to overcome resistance. We observed enzalutamide resistance in bone lesion development induced by PCa cells in mouse models. We found that the bone microenvironment was indispensable for enzalutamide resistance because enzalutamide significantly inhibited the growth of subcutaneous C4-2B tumors and the proliferation of C4-2B cells isolated from the bone lesions, and the resistance was recapitulated only when C4-2B cells were co-cultured with osteoblasts. In revealing how osteoblasts contribute to enzalutamide resistance, we found that enzalutamide decreased TGFBR2 protein expression in osteoblasts, which was supported by clinical data. This decrease was possibly through PTH1R-mediated endocytosis. We showed that PTH1R blockade rescued enzalutamide-mediated decrease in TGFBR2 levels and enzalutamide responses in C4-2B cells that were co-cultured with osteoblasts. This is the first study to reveal the contribution of the bone microenvironment to enzalutamide resistance and identify PTH1R as a feasible target to overcome the resistance in PCa bone metastases.

Keywords

enzalutamide resistance; prostate cancer; bone microenvironment; TGFBR2; PTH1R

1. Introduction

Enzalutamide, a second-generation small-molecule inhibitor of the androgen receptor (AR), has been approved for patients with metastatic castration-resistant prostate cancer (PCa) (mCRPC) after androgen deprivation therapy failure [1–3]. However, resistance develops within six months in patients with initial responses [4–9]. In addition, the bone is the most frequent site for PCa metastases, as nearly 90% of patients die from bone metastases [10]. Therefore, there is an urgent need to overcome enzalutamide resistance in PCa bone metastases.

Although various mechanisms of enzalutamide resistance have been identified [4, 5, 8, 9, 11], targeting only cancer cells is unlikely to achieve the goal of overcoming drug resistance due to the heterogeneity and plasticity/evolution of the cancer cell population. In contrast, the microenvironment influences not only cancer initiation, progression, and metastases, but also treatment responses [12–24]. However, the systematic effects of the tumor microenvironment on drug resistance have not received significant attention. Therefore, we aimed to determine whether and how the effect of enzalutamide on the bone microenvironment contributes to PCa bone metastases and drug resistance.

The bone microenvironment, the “soil” for the PCa cell seeds that disseminate to the bone, consists of various types of cells, including osteoblasts (bone-forming cells) and osteoclasts (bone-absorbing cells). In PCa bone metastases, osteoblasts provide niches for PCa cell colonization and progression to overt metastases [25–31]. We found that enzalutamide treatment significantly inhibited C4-2B subcutaneous tumor growth, but not C4-2B induced bone lesion development. Similar results were observed when another AR-positive PCa cell

line VCaP was used. No differences were observed between cultured C4-2B cells sorted from subcutaneous and bone lesions, in terms of cell proliferation *per se* and enzalutamide-inhibited cell viability, suggesting that the bone microenvironment may confer enzalutamide resistance in PCa bone metastases. We also observed enzalutamide resistance in C4-2B cells co-cultured with osteoblasts, but not with fibroblasts or mesenchymal stem cells, suggesting a potential specific role of osteoblasts in the observed enzalutamide resistance. Using PCa bone metastatic tissue microarray, we found lower TGFBR2 expression levels in osteoblasts in patients treated with enzalutamide or abiraterone. In cultured MC3T3-E1 osteoblasts, we also observed that enzalutamide significantly decreased the expression of TGFBR2 at protein level, but not at the transcription level, in a dose- and time-dependent manner. In a genetically engineered mouse model, we found that *Tgfbr2* knockout in osteoblasts promoted C4-2B cell-induced bone lesion development and the incidence of bone lesions. Lastly, we determined the mechanism by which enzalutamide-induced decrease in the TGFBR2 level in osteoblasts was mediated by PTH1R (parathyroid hormone/parathyroid hormone-related peptide receptor), possibly through endocytosis. Blocking PTH1R activity rescued enzalutamide-induced TGFBR2 loss in osteoblasts and helped in overcoming enzalutamide resistance in the co-culture system of C4-2B and MC3T3-E1 cells. Our findings suggest a novel enzalutamide resistance mechanism through PTH1R-mediated decrease in the TGFBR2 level in osteoblasts and that blocking PTH1R might overcome enzalutamide resistance in PCa bone metastases.

2. Materials and Methods

The full materials and methods, including cell lines, reagents, and protocols, can be found in the Supplementary Data.

2.1 Mouse models

The genetically engineered mouse models, $Tgfbr2^{FloxE2}$ and $Tgfbr2^{Col1CreERT}$ knockout (KO), used in the present study have been characterized and described previously [19]. In this study, the mice were crossed with the NSG-SCID (NOD.Cg-Prkdcscid Il2rgtm1Wjl/SzJ) mouse background and confirmed to be immunodeficient at IgG levels for human PCa cells to grow in the bones. The research protocols using these Tgfbr2 engineered mice and NSG-SCID were approved by the Institutional Animal Care and Use Committee under protocol numbers 19-01-002/10-01-001 at Van Andel Institute and 400066/400067 at the University of Toledo.

2.2 *In vitro* co-culture

For co-culture, C4-2B/GFP cells were seeded simultaneously with MC3T3-E1, NIH3T3, or OP-9 cells at a 1:1 ratio at a density of 5,000 cells (2,500 cells each per well) in 48-well plates, in triplicate for each group. The mono-cultures of C4-2B/GFP cells were performed in 48-well plates at a density of 2,500 cells per well, to control the drug response. The cells were treated with various concentrations of the drugs or vehicle (dimethyl sulfoxide, DMSO). Fluorescence images and bright-field images at 10X magnitude were taken daily. The fluorescence areas in each image were quantified and normalized to the values of the

starting images in each group to obtain the relative confluency ratios. Plots were generated using GraphPad Prism v8.0 (GraphPad Software Inc, San Diego, CA, USA).

2.3 Statistical analysis

Lesion and tumor growth rates were analyzed using linear mixed-effects models with random slopes and intercepts per animal to account for repeated measures. Data were transformed as needed to better meet normality and homoscedasticity assumptions. For bone lesion proportion analysis, a two-sample proportion test was performed. For bone lesion area comparison, in the tibiae of $Tgfbr2^{Col1CreERT}$ KO and $Tgfbr2^{FloxE2}$ mice, we performed the Wilcoxon rank-sum test with continuity correction and applied the Bonferroni-Holm multiple test correction. The drug response and cell viability results were analyzed using the Wilcoxon rank-sum test, followed by Fisher's combined probability test. For *in vitro* co-culture and quantitative reverse transcription polymerase chain reaction (qRT-PCR) results, the Welch t-test was used. All analyses were performed using R v 3.2.2 and statistical significance was set at $p < 0.05$.

3. Results

3.1 Enzalutamide resistance in C4-2B bone metastases is dependent on bone microenvironment

We injected AR-positive PCa C4-2B cells (1 million cells per injection) into the subcutaneous flank regions (Fig. 1A) or tibiae (Fig. 1B) of male NSG-SCID mice (5–6 week old). Enzalutamide (20 mg/kg body weight) or vehicle was administered daily by oral gavage for 2 to 3 consecutive weeks when most of the subcutaneous tumors reached 100 mm^3 in size (starting from day 21 in the subcutaneous model) or day 1 post C4-2B cell injection in the intratibial model. The dosing was chosen based on the reported C_{max} in previous studies [32–35]. Consistent with a previous report [36], enzalutamide treatment significantly inhibited C4-2B tumor growth in subcutaneous xenografts in two independent experiments (Fig. 1A). However, enzalutamide treatment had no effect on the C4-2B-induced bone lesion development (Fig. 1B). Similarly, enzalutamide inhibited subcutaneous tumor growth but not bone lesion development in the model of VCaP, another CRPC line (Supplementary Fig. S1A, B). Together, these data showed that enzalutamide resistance developed in PCa cells xenografted into the bone microenvironment.

To test whether the lack of enzalutamide response was due to the functional evolution of C4-2B cells or the context of the bone microenvironment, we isolated the GFP-labeled C4-2B cells from the subcutaneous tumors (C4-2B_subQ) or bone metastases (C4-2B_bone) by flow cytometry and cultured them for no more than three generations before testing. We found no difference in cell proliferation between C4-2B_subQ and C4-2B_bone (Fig. 1C, upper panel). We further treated the cells with enzalutamide and observed no difference in cell viability between C4-2B_subQ and C4-2B_bone(Fig. 1C, lower panel). These data suggest that enzalutamide resistance is not intrinsic to PCa cells, but is dependent on the context of the bone microenvironment, which likely causes enzalutamide resistance in bone metastases.

3.2 Enzalutamide decreases TGFBR2 level in osteoblasts resulting in enzalutamide resistance in C4-2B cells

Using a set of mCRPC patient tissue microarrays (UWTMA79) supported by the Prostate Cancer Biorepository Network, the immunohistochemical analysis of TGFBR2 was performed. We found that the expression scores of TGFBR2 in osteoblasts were significantly lower in patients who had received second-line AR signaling blockers (n = 13, enzalutamide or abiraterone, an androgen biosynthesis inhibitor [37]) than in those who did not receive enzalutamide or abiraterone (n = 32) (Fig. 2A, B). No correlations were found between TGFBR2 expression in osteoblasts and any other treatment group (such as bisphosphonate medicine Zometa, or antifungal reagent ketoconazole) or between TGFBR2 expression in other cell types (such as tumor cells, stromal/fibroblasts, or osteoclasts) and any treatments (Supplementary Table 1, Supplementary Fig. S2A–C).

We compared the effect of enzalutamide on C4-2B cells cultured alone or co-cultured with mouse osteoblasts MC3T3-E1, fibroblasts NIH3T3, or mesenchymal stem cells OP-9. We found that enzalutamide significantly inhibited the growth of C4-2B cells that were cultured alone (mono-culture), or co-cultured with NIH3T3 fibroblasts or OP-9 mesenchymal progenitor cells (Fig. 1D and Supplementary Fig. S3). However, when co-cultured with MC3T3-E1 cells, C4-2B cells did not respond to enzalutamide at doses of 10 μM and 20 μM. The average relative cell confluency of C4-2B at day 4 post 40 μM enzalutamide treatment compared to that of vehicle-treated group was 70% in MC3T3-E1 co-culture whereas the corresponding confluency was 47%, 43%, and 55% in C4-2B mono-culture, NIH3T3 co-culture and OP-9 co-culture, respectively, suggesting less C4-2B cell responses to enzalutamide even at high doses when co-cultured with osteoblasts (Fig. 1D). Altogether, these data suggest the key role of osteoblasts in the enzalutamide resistance of C4-2B bone metastases, possibly through a decrease in the TGFBR2 level.

We treated MC3T3-E1 osteoblasts with enzalutamide and found that enzalutamide significantly decreased the level of TGFBR2 protein, at 24 to 72 h, at 20 μM and 40 μM doses. Enzalutamide at 40 μM also decreased the TGFBR2 levels at 8 h and 12 h time points. No effects were observed upon 6 h of the treatment (Fig. 2C). Decreases in TGFBR2 levels were also observed in a human fetal osteoblast cell line, hFOB1.19, and primary cultured mouse osteoblasts differentiated from bone marrow (Supplementary Fig. S4A, B). To rule out the non-specific effect of enzalutamide as a small molecule, we knocked down *Ar* in MC3T3-E1 osteoblasts and observed a consistent decrease in the TGFBR2 level (Fig. 2D), suggesting the on-target effect of enzalutamide. Altogether, these data suggest that blocking AR signaling with enzalutamide can decrease TGFBR2 expression in osteoblasts, and that the decrease in TGFBR2 level in osteoblasts results in the enzalutamide resistance of C4-2B bone metastases.

3.3 Deletion of *Tgfbr2* in osteoblasts promotes C4-2B bone metastases

The loss of TGFBR2 in osteoblasts promotes the bone metastases of AR-negative CRPC cells, such as PC-3 and DU145 [19]. To determine the function of TGFBR2 in osteoblasts in AR-positive C4-2B bone metastases, we injected C4-2B cells into the tibiae of the floxed control mice and the previously established mouse model $Tgfbr2^{Col1CreERT}$ KO mice, in

which *Tgfbr2* was specifically knocked out in osteoblasts after tamoxifen induction [19]. We found that 21 out of 24 injected mouse tibiae developed C4-2B cell-induced bone lesions in the $Tgfbr2^{Col1CreERT}$ KO group, whereas only 7 out of 18 injected mouse tibiae developed bone lesions in the $Tgfbr2^{FloxE2}$ (control) group (Fig. 3A). The proportions of the incidence of bone lesions in the two groups were significantly different in the two-sample proportion test. We also found that the knockout group had a significantly greater bone lesion area (median = 3.4996) than the control group (median = 0) at week 5 post-injection (Fig. 3B). These data suggested that the loss of TGFBR2 in osteoblasts promoted the bone metastases of AR-positive CRPC cells and possibly caused enzalutamide resistance.

3.4 Enzalutamide decreases TGFBR2 level through PTH1R-endocytosis-lysosome pathway

The mRNA levels of *Tgfbr2* did not significantly change after enzalutamide treatment in MC3T3-E1 cells (Supplementary Fig. S5), suggesting that the TGFBR2 level in osteoblasts decreased because of post-translational regulation, such as protein degradation. As proteasomes and lysosomes are the final destinations for protein degradation, we treated MC3T3-E1 cells with enzalutamide for 24 h and introduced inhibitors of proteasome (MG132, carfilzomib, and bortezomib) and autophagy/lysosome (chloroquine and bafilomycin A) at different time points (Fig. 4A). We found that TGFBR2 levels were significantly decreased by all three proteasomal inhibitors, suggesting that TGFBR2 loss induced by enzalutamide was not dependent on functional proteosomes (Fig. 4B, C). Autophagy/lysosome inhibitors, chloroquine or bafilomycin A, induced increases in TGFBR2 and rescued TGFBR2 in the presence of enzalutamide to the level of the vehicle-treated group (Fig. 4D, E), suggesting that TGFBR2 protein levels, under normal and enzalutamide-regulated conditions, were partially controlled by lysosomes and lysosomal degradation.

A previous study revealed that parathyroid hormone (PTH) activates PTH1R to recruit TGFBR2, which phosphorylates PTH1R and undergoes endocytosis together with PTH1R for protein degradation [38]. PTH1R is the only known receptor for parathyroid hormone-related protein (PTHrP), which is highly expressed and secreted by PCa cells [39, 40]. To test whether endogenous TGFBR2 and PTH1R also interact and go through the endocytosis pathway when enzalutamide treatment was administered, we used two dynamin inhibitors, dynasore and Dyngo-4a, to block endocytosis in osteoblasts [41, 42]. Indeed, blocking endocytosis rescued the decrease in the TGFBR2 level when the enzalutamide treatment was administered (Fig. 4C, F). Combined treatment with bafilomycin A and dynasore completely inhibited TGFBR2 loss after enzalutamide treatment (Fig. 4F). These data suggest that enzalutamide-induced TGFBR2 loss is dependent on endocytosis.

We found that enzalutamide treatment increased PTH1R expression before the decrease in TGFBR2 levels (Fig. 5A). PTH1R protein levels were increased after enzalutamide treatment at multiple time points from 2 to 24 h but were not affected at 48 h. The most significant increase in PTH1R levels was observed at 6 h, when there was no change in the levels of TGFBR2. The down-regulation of TGFBR2 expression was consistently observed at and after 24 h of treatment. These data suggested that enzalutamide induced

the expression of PTH1R, which may subsequently cause a decrease in the TGFBR2 level via endocytosis. Furthermore, we treated C4-2B cells stably over-expressing TGFBR2 (termed as C4-2B/TGFBR2, C4-2B cells have very low endogenous TGFBR2 levels [43]) or osteoclast RAW264.7 cells with enzalutamide and found that the PTH1R level was not increased, although the TGFBR2 level was decreased at certain time points (Supplementary Fig. S6A–C). These data suggest that the enzalutamide-induced PTH1R-mediated decrease in TGFBR2 level was specific to osteoblasts. We then applied a peptide antagonist of PTH1R, (Asn^{10}, Leu^{11}, and D-Trp^{12}) PTHrP (7–34) amide at a concentration of 100 ng/μL to block PTH1R activation and observed the rescue of TGFBR2 loss (Fig. 5B, C). Importantly, we found that blocking PTH1R restored the growth inhibition caused by enzalutamide in C4-2B and MC3T3-E1 co-culture (Fig. 5D).

3.5 Enzalutamide increases NR2F1 binding to *Pth1r* promoter

Using qRT-PCR, we observed that enzalutamide significantly increased the levels of *Pth1r* mRNA at early time points (1 h, 2 h, 4 h, and 6 h) (Fig. 6A). These data suggest regulation at the transcriptional level. We used a text-mining approach called MetaCore to search for candidates that are linked with both AR and PTH1R and found that the top hit was nuclear receptor subfamily 2 group F member 1 (NR2F1). NR2F1 is negatively associated with AR signaling and can activate the expression of *Pth1r* [44, 45]. We found that enzalutamide significantly increased NR2F1 at both mRNA (1 h, 2 h, and 4 h treatment) (Fig. 6B) and protein levels (Fig. 6C) in osteoblasts. No increase in NR2F1 levels was observed in either RAW264.7 or C4-2B/TGFBR2 cells (Supplementary Fig. S6A, B). We downloaded the binding element information of NR2F1 (5'-A/G-A/G-GGTCA-3') from the JASPAR database and searched the elements across the upstream regulatory sequences of mouse *Pth1r* (Fig. 6D) [46]. There are at least three major transcript variants of mouse *Pth1r* (labeled as V1, V2, and V3, driven by at least three different promoters); the promoter of V1 (containing exons E1, E2, E4, and those follow) is considered absent or very weak in the bone, whereas those of V2 (containing E3, E4, and those follow) and V3 (containing E4', E4, and those follow) are active in the bone [47]. We found multiple NR2F1 binding elements at the promoters of V2 and V3. We conducted ChIP-qPCR (primer amplicons termed as p1 for V2 and p2 for V3) and found that NR2F1 bound to both designed promoter regions and enzalutamide enhanced these bindings (Fig. 6D). These data suggest that enzalutamide directly induces *Pth1r* transcription by enhancing NR2F1 occupancy on the *Pth1r* promoter.

4. Discussion

Enzalutamide resistance is common in patients with PCa bone metastases. Various resistance mechanisms have been and are continuously being revealed and studied [5, 48–50]. In this study, we observed enzalutamide resistance in bone lesion development induced by PCa C4-2B and VCaP cells in a mouse model. Enzalutamide resistance was not observed in subcutaneously injected C4-2B tumors or in the C4-2B cells isolated from the bone lesions but was recapitulated only when C4-2B cells were co-cultured with osteoblasts, suggesting a dispensable role of the bone microenvironment in enzalutamide resistance. To reveal how the bone microenvironment contributes to enzalutamide resistance, we first searched

for clinical relevance. Using PCa bone metastatic tissue microarray, we found that the samples from patients receiving enzalutamide or abiraterone treatment had lower TGFBR2 expression in osteoblasts. Further, we determined the links between enzalutamide resistance and TGFBR2 protein expression in osteoblasts. We found that enzalutamide treatment decreased TGFBR2 protein expression in osteoblasts in a dose- and time-dependent manner. This decrease was mediated by PTH1R-mediated endocytosis and subsequent degradation. Enzalutamide induced the transcription of *Pth1r* mRNA, possibly through enhanced NR2F1 occupancy on the *Pth1r* promoter. Importantly, PTH1R blockade rescued the enzalutamide-induced decrease in TGFBR2 levels and the enzalutamide response of C4-2B cells that were co-cultured with osteoblasts. To the best of our understanding, this is the first study to reveal the contribution of the bone microenvironment, specifically the osteoblasts, to enzalutamide resistance and that the key factor PTH1R has a therapeutic potential against enzalutamide resistance.

There are several possibilities for enzalutamide resistance observed in bone metastases. For example, 1) the evolution of metastasized PCa cells in the bone microenvironment, 2) the delivery of enzalutamide to the bone, 3) the physical drug absorption/competition by stromal cells in the bone, or 4) the effects of cells from the bone microenvironment. To rule out some of these possibilities, we first isolated C4-2B cells from either subcutaneous or intratibial xenografts and observed no significant differences in cell proliferation and enzalutamide responses. Second, a pharmacokinetic study in rats showed that the detectable enzalutamide and its active metabolites were similar between bone marrow and other tissues such as the prostate [51]. Third, using an *in vitro* co-culture model, we found the enzalutamide resistance of C4-2B cells only in the co-cultures of osteoblasts but not in those of NIH3T3 fibroblasts or mesenchymal progenitor OP-9 cells. Therefore, we focused on the roles and effects of osteoblasts. Notably, we used the mouse osteoblasts for the co-culture because the optimal culture temperature for the human osteoblast cell line hFOB1.19 is 34°C, which is not same for PCa cells (37°C), and primary human osteoblasts are difficult to obtain. We showed that enzalutamide treatment decreased TGFBR2 levels in osteoblasts in a time- and dose-dependent manner. Importantly, clinical data showed a decreased TGFBR2 expression only in osteoblasts in PCa bone metastatic patients who received enzalutamide or abiraterone treatment but failed, supporting the hypothesis that enzalutamide decreases TGFBR2 expression in osteoblasts and that this decrease causes drug resistance in PCa bone metastases. Although we recognized the limitations of this piece of clinical data, including the small sample size, the samples obtained from one center only, the subjectivity of the pathological readings, and the limitations of studies on decalcified tissues with bones, including the unsuccessful IHC of several important proteins, such as PTH1R and NR2F1, in our hands, the data we obtained from *in vitro* studies supported our hypothesis.

In this study, we found that the enzalutamide-NR2F1-PTH1R-TGFBR2 axis is specific to osteoblasts, but not PCa cells or osteoclasts, the other two major types of cells in bone metastases. This is important because the loss of TGFBR2 or blockade of TGF-β signaling in either myeloid lineage cells or cancer cells inhibited cancer metastases; only the loss of TGFBR2 in osteoblasts promoted PCa bone metastases (including C4-2B bone metastases shown in this study) [17, 19, 20, 52, 53]. Therefore, targeting PTH1R is osteoblast-specific. In contrast, PTHrP secreted from cancer cells activates PTH1R expression [54]. Blocking

PTHrP using neutralizing antibodies has been shown to be effective in preclinical bone metastasis prevention studies [55]. Altogether, blocking PTH1R is potentially effective and needs to be further tested in the context of overcoming enzalutamide resistance. PTH1R belongs to the family of G-protein coupled receptors, which are targets for approximately 35% of currently approved drugs [56].

We showed that the TGFBR2 expression decreased by enzalutamide in osteoblasts within 2 days, and enzalutamide resistance was observed after 3 days of C4-2B co-culture with osteoblasts *in vitro*. The time needed for enzalutamide resistant PCa clones to develop *in vitro* or *in vivo* was 2–3 days, which is much shorter than weeks or months [57–59]. Therefore, effectively targeting PTH1R to overcome enzalutamide resistance in mCRPC can prevent and eliminate the evolution of PCa cells to acquire resistance. Our future studies will explore the effectiveness and toxicity of the combination treatment of enzalutamide and PTH1R inhibition *in vivo*, as well as develop and test novel approaches to PTH1R inhibition.

Supplementary Material

Refer to Web version on PubMed Central for supplementary material.

Acknowledgments

We thank David Nadziejka for technical editing and Editage (www.editage.com) for English language editing. This work was supported by NCI grant R01CA230744 and a grant from Van Andel Institute (50310A) to XL. The prostate cancer bone metastases tissue microarray was purchased from the Prostate Cancer Biorepository Network (funded by W81XWH-14-2-0182, W81XWH-14-2-0183, W81XWH-14-2-0185, W81XWH-14-2-0186, and W81XWH-15-2-0062).

Financial support:

This work was supported by National Cancer Institute (R01CA230744) granted to Xiaohong Li.

References

[1]. Tran C, Ouk S, Clegg NJ, Chen Y, Watson PA, Arora V, Wongvipat J, Smith-Jones PM, Yoo D, Kwon A, Wasielewska T, Welsbie D, Chen CD, Higano CS, Beer TM, Hung DT, Scher HI, Jung ME, Sawyers CL, Development of a second-generation antiandrogen for treatment of advanced prostate cancer, Science, 324 (2009) 787–790. [PubMed: 19359544]

[2]. Beer TM, Armstrong AJ, Rathkopf DE, Loriot Y, Sternberg CN, Higano CS, Iversen P, Bhattacharya S, Carles J, Chowdhury S, Davis ID, de Bono JS, Evans CP, Fizazi K, Joshua AM, Kim CS, Kimura G, Mainwaring P, Mansbach H, Miller K, Noonberg SB, Perabo F, Phung D, Saad F, Scher HI, Taplin ME, Venner PM, Tombal B, P. Investigators, Enzalutamide in metastatic prostate cancer before chemotherapy, N Engl J Med, 371 (2014) 424–433. [PubMed: 24881730]

[3]. Scher HI, Fizazi K, Saad F, Taplin ME, Sternberg CN, Miller K, de Wit R, Mulders P, Chi KN, Shore ND, Armstrong AJ, Flaig TW, Flechon A, Mainwaring P, Fleming M, Hainsworth JD, Hirmand M, Selby B, Seely L, de Bono JS, A. Investigators, Increased survival with enzalutamide in prostate cancer after chemotherapy, N Engl J Med, 367 (2012) 1187–1197. [PubMed: 22894553]

[4]. Efstathiou E, Titus M, Wen S, Hoang A, Karlou M, Ashe R, Tu SM, Aparicio A, Troncoso P, Mohler J, Logothetis CJ, Molecular characterization of enzalutamide-treated bone metastatic castration-resistant prostate cancer, Eur Urol, 67 (2015) 53–60. [PubMed: 24882673]

[5]. Vander Ark A, Cao J, Li X, Mechanisms and Approaches for Overcoming Enzalutamide Resistance in Prostate Cancer, Front Oncol, 8 (2018) 180. [PubMed: 29911070]

[6]. McCain J, Drugs that offer a survival advantage for men with bone metastases resulting from castration-resistant prostate cancer: new and emerging treatment options, P & T : a peer-reviewed journal for formulary management, 39 (2014) 130–143. [PubMed: 24669181]

[7]. Merseburger AS, Haas GP, von Klot CA, An update on enzalutamide in the treatment of prostate cancer, Therapeutic advances in urology, 7 (2015) 9–21. [PubMed: 25642291]

[8]. Culig Z, Molecular Mechanisms of Enzalutamide Resistance in Prostate Cancer, Curr Mol Biol Rep, 3 (2017) 230–235. [PubMed: 29214142]

[9]. Tucci M, Zichi C, Buttigliero C, Vignani F, Scagliotti GV, Di Maio M, Enzalutamide-resistant castration-resistant prostate cancer: challenges and solutions, Onco Targets Ther, 11 (2018) 7353–7368. [PubMed: 30425524]

[10]. Bubendorf L, Schopfer A, Wagner U, Sauter G, Moch H, Willi N, Gasser TC, Mihatsch MJ, Metastatic patterns of prostate cancer: an autopsy study of 1,589 patients, Hum Pathol, 31 (2000) 578–583. [PubMed: 10836297]

[11]. Yuan X, Cai C, Chen S, Chen S, Yu Z, Balk SP, Androgen receptor functions in castration-resistant prostate cancer and mechanisms of resistance to new agents targeting the androgen axis, Oncogene, 33 (2014) 2815–2825. [PubMed: 23752196]

[12]. Bhowmick NA, Chytil A, Plieth D, Gorska AE, Dumont N, Shappell S, Washington MK, Neilson EG, Moses HL, TGF-beta signaling in fibroblasts modulates the oncogenic potential of adjacent epithelia, Science, 303 (2004) 848–851. [PubMed: 14764882]

[13]. Kim BG, Li C, Qiao W, Mamura M, Kasprzak B, Anver M, Wolfraim L, Hong S, Mushinski E, Potter M, Kim SJ, Fu XY, Deng C, Letterio JJ, Smad4 signalling in T cells is required for suppression of gastrointestinal cancer, Nature, 441 (2006) 1015–1019. [PubMed: 16791201]

[14]. Hahn JN, Falck VG, Jirik FR, Smad4 deficiency in T cells leads to the Th17-associated development of premalignant gastroduodenal lesions in mice, J Clin Invest, 121 (2011) 4030–4042. [PubMed: 21881210]

[15]. Li X, Placencio V, Iturregui JM, Uwamariya C, Sharif-Afshar AR, Koyama T, Hayward SW, Bhowmick NA, Prostate tumor progression is mediated by a paracrine TGF-beta/Wnt3a signaling axis, Oncogene, 27 (2008) 7118–7130. [PubMed: 18724388]

[16]. Li X, Sterling JA, Fan KH, Vessella RL, Shyr Y, Hayward SW, Matrisian LM, Bhowmick NA, Loss of TGF-beta responsiveness in prostate stromal cells alters chemokine levels and facilitates the development of mixed osteoblastic/osteolytic bone lesions, Molecular cancer research : MCR, 10 (2012) 494–503. [PubMed: 22290877]

[17]. Pang Y, Gara SK, Achyut BR, Li Z, Yan HH, Day CP, Weiss JM, Trinchieri G, Morris JC, Yang L, TGF-beta signaling in myeloid cells is required for tumor metastasis, Cancer discovery, 3 (2013) 936–951. [PubMed: 23661553]

[18]. Calon A, Espinet E, Palomo-Ponce S, Tauriello DV, Iglesias M, Cespedes MV, Sevillano M, Nadal C, Jung P, Zhang XH, Byrom D, Riera A, Rossell D, Mangues R, Massague J, Sancho E, Batlle E, Dependency of colorectal cancer on a TGF-beta-driven program in stromal cells for metastasis initiation, Cancer Cell, 22 (2012) 571–584. [PubMed: 23153532]

[19]. Meng X, Vander Ark A, Daft P, Woodford E, Wang J, Madaj Z, Li X, Loss of TGF-beta signaling in osteoblasts increases basic-FGF and promotes prostate cancer bone metastasis, Cancer Lett, 418 (2018) 109–118. [PubMed: 29337106]

[20]. Meng X, Vander Ark A, Lee P, Hostetter G, Bhowmick NA, Matrisian LM, Williams BO, Miranti CK, Li X, Myeloid-specific TGF-beta signaling in bone promotes basic-FGF and breast cancer bone metastasis, Oncogene, 35 (2016) 2370–2378. [PubMed: 26279296]

[21]. Zhang XH, Jin X, Malladi S, Zou Y, Wen YH, Brogi E, Smid M, Foekens JA, Massague J, Selection of bone metastasis seeds by mesenchymal signals in the primary tumor stroma, Cell, 154 (2013) 1060–1073. [PubMed: 23993096]

[22]. Valencia T, Kim JY, Abu-Baker S, Moscat-Pardos J, Ahn CS, Reina-Campos M, Duran A, Castilla EA, Metallo CM, Diaz-Meco MT, Moscat J, Metabolic reprogramming of stromal fibroblasts through p62-mTORC1 signaling promotes inflammation and tumorigenesis, Cancer Cell, 26 (2014) 121–135. [PubMed: 25002027]

[23]. Jiao S, Subudhi SK, Aparicio A, Ge Z, Guan B, Miura Y, Sharma P, Differences in Tumor Microenvironment Dictate T Helper Lineage Polarization and Response to Immune Checkpoint Therapy, Cell, 179 (2019) 1177–1190. [PubMed: 31730856]

[24]. Binnewies M, Roberts EW, Kersten K, Chan V, Fearon DF, Merad M, Coussens LM, Gabrilovich DI, Ostrand-Rosenberg S, Hedrick CC, Vonderheide RH, Pittet MJ, Jain RK, Zou W, Howcroft TK, Woodhouse EC, Weinberg RA, Krummel MF, Understanding the tumor immune microenvironment (TIME) for effective therapy, Nat Med, 24 (2018) 541–550. [PubMed: 29686425]

[25]. Lam HM, Vessella RL, Morrissey C, The role of the microenvironment-dormant prostate disseminated tumor cells in the bone marrow, Drug Discov Today Technol, 11 (2014) 41–47. [PubMed: 24847652]

[26]. Lawson MA, McDonald MM, Kovacic N, Hua Khoo W, Terry RL, Down J, Kaplan W, Paton-Hough J, Fellows C, Pettitt JA, Neil Dear T, Van Valckenborgh E, Baldock PA, Rogers MJ, Eaton CL, Vanderkerken K, Pettit AR, Quinn JM, Zannettino AC, Phan TG, Croucher PI, Osteoclasts control reactivation of dormant myeloma cells by remodelling the endosteal niche, Nat Commun, 6 (2015) 8983. [PubMed: 26632274]

[27]. Pedersen EA, Shiozawa Y, Pienta KJ, Taichman RS, The prostate cancer bone marrow niche: more than just 'fertile soil', Asian journal of andrology, 14 (2012) 423–427. [PubMed: 22367179]

[28]. Schuettpelz LG, Link DC, Niche competition and cancer metastasis to bone, The Journal of clinical investigation, 121 (2011) 1253–1255. [PubMed: 21436576]

[29]. Shiozawa Y, Havens AM, Jung Y, Ziegler AM, Pedersen EA, Wang J, Lu G, Roodman GD, Loberg RD, Pienta KJ, Taichman RS, Annexin II/annexin II receptor axis regulates adhesion, migration, homing, and growth of prostate cancer, Journal of cellular biochemistry, 105 (2008) 370–380. [PubMed: 18636554]

[30]. Shiozawa Y, Pedersen EA, Havens AM, Jung Y, Mishra A, Joseph J, Kim JK, Patel LR, Ying C, Ziegler AM, Pienta MJ, Song J, Wang J, Loberg RD, Krebsbach PH, Pienta KJ, Taichman RS, Human prostate cancer metastases target the hematopoietic stem cell niche to establish footholds in mouse bone marrow, The Journal of clinical investigation, 121 (2011) 1298–1312. [PubMed: 21436587]

[31]. Shiozawa Y, Pedersen EA, Patel LR, Ziegler AM, Havens AM, Jung Y, Wang J, Zalucha S, Loberg RD, Pienta KJ, Taichman RS, GAS6/AXL axis regulates prostate cancer invasion, proliferation, and survival in the bone marrow niche, Neoplasia, 12 (2010) 116–127. [PubMed: 20126470]

[32]. Borgmann H, Lallous N, Ozistanbullu D, Beraldi E, Paul N, Dalal K, Fazli L, Haferkamp A, Lejeune P, Cherkasov A, Gleave ME, Moving Towards Precision Urologic Oncology: Targeting Enzalutamide-resistant Prostate Cancer and Mutated Forms of the Androgen Receptor Using the Novel Inhibitor Darolutamide (ODM-201), Eur Urol, 73 (2018) 4–8. [PubMed: 28851578]

[33]. Guerrero J, Alfaro IE, Gomez F, Protter AA, Bernales S, Enzalutamide, an androgen receptor signaling inhibitor, induces tumor regression in a mouse model of castration-resistant prostate cancer, The Prostate, 73 (2013) 1291–1305. [PubMed: 23765603]

[34]. Liu C, Lou W, Zhu Y, Yang JC, Nadiminty N, Gaikwad NW, Evans CP, Gao AC, Intracrine Androgens and AKR1C3 Activation Confer Resistance to Enzalutamide in Prostate Cancer, Cancer research, 75 (2015) 1413–1422. [PubMed: 25649766]

[35]. CHMP, CHMP assessment report for Xtandi (enzalutamide), 2013.

[36]. Liu C, Armstrong C, Zhu Y, Lou W, Gao AC, Niclosamide enhances abiraterone treatment via inhibition of androgen receptor variants in castration resistant prostate cancer, Oncotarget, 7 (2016) 32210–32220. [PubMed: 27049719]

[37]. Rehman Y, Rosenberg JE, Abiraterone acetate: oral androgen biosynthesis inhibitor for treatment of castration-resistant prostate cancer, Drug Des Devel Ther, 6 (2012) 13–18.

[38]. Qiu T, Wu X, Zhang F, Clemens TL, Wan M, Cao X, TGF-beta type II receptor phosphorylates PTH receptor to integrate bone remodelling signalling, Nature cell biology, 12 (2010) 224–234. [PubMed: 20139972]

[39]. Wysolmerski JJ, Parathyroid hormone-related protein: an update, J Clin Endocrinol Metab, 97 (2012) 2947–2956. [PubMed: 22745236]

[40]. Pioszak AA, Parker NR, Gardella TJ, Xu HE, Structural basis for parathyroid hormone-related protein binding to the parathyroid hormone receptor and design of conformation-selective peptides, The Journal of biological chemistry, 284 (2009) 28382–28391. [PubMed: 19674967]

[41]. McCluskey A, Daniel JA, Hadzic G, Chau N, Clayton EL, Mariana A, Whiting A, Gorgani NN, Lloyd J, Quan A, Moshkanbaryans L, Krishnan S, Perera S, Chircop M, von Kleist L, McGeachie AB, Howes MT, Parton RG, Campbell M, Sakoff JA, Wang X, Sun JY, Robertson MJ, Deane FM, Nguyen TH, Meunier FA, Cousin MA, Robinson PJ, Building a better dynasore: the dyngo compounds potently inhibit dynamin and endocytosis, Traffic, 14 (2013) 1272–1289. [PubMed: 24025110]

[42]. Kirchhausen T, Macia E, Pelish HE, Use of dynasore, the small molecule inhibitor of dynamin, in the regulation of endocytosis, Methods Enzymol, 438 (2008) 77–93. [PubMed: 18413242]

[43]. Song B, Park SH, Zhao JC, Fong KW, Li S, Lee Y, Yang YA, Sridhar S, Lu X, Abdulkadir SA, Vessella RL, Morrissey C, Kuzel TM, Catalona W, Yang X, Yu J, Targeting FOXA1-mediated repression of TGF-beta signaling suppresses castration-resistant prostate cancer progression, J Clin Invest, 129 (2019) 569–582. [PubMed: 30511964]

[44]. Karperien M, Farih-Sips H, Hendriks JA, Lanske B, Papapoulos SE, Abou-Samra AB, Lowik CW, Defize LH, Identification of a retinoic acid-inducible element in the murine PTH/PTHrP (parathyroid hormone/parathyroid hormone-related peptide) receptor gene, Mol Endocrinol, 13 (1999) 1183–1196. [PubMed: 10406468]

[45]. Perets R, Kaplan T, Stein I, Hidas G, Tayeb S, Avraham E, Ben-Neriah Y, Simon I, Pikarsky E, Genome-wide analysis of androgen receptor targets reveals COUP-TF1 as a novel player in human prostate cancer, PLoS One, 7 (2012) e46467. [PubMed: 23056316]

[46]. Khan A, Fornes O, Stigliani A, Gheorghe M, Castro-Mondragon JA, van der Lee R, Bessy A, Cheneby J, Kulkarni SR, Tan G, Baranasic D, Arenillas DJ, Sandelin A, Vandepoele K, Lenhard B, Ballester B, Wasserman WW, Parcy F, Mathelier A, JASPAR 2018: update of the open-access database of transcription factor binding profiles and its web framework, Nucleic Acids Res, 46 (2018) D260–D266. [PubMed: 29140473]

[47]. Kawane T, Mimura J, Fujii-Kuriyama Y, Horiuchi N, Identification of the promoter region of the parathyroid hormone receptor gene responsible for transcriptional suppression by insulin-like growth factor-I, Arch Biochem Biophys, 439 (2005) 61–69. [PubMed: 15950922]

[48]. Alumkal JJ, Sun D, Lu E, Beer TM, Thomas GV, Latour E, Aggarwal R, Cetnar J, Ryan CJ, Tabatabaei S, Bailey S, Turina CB, Quigley DA, Guan X, Foye A, Youngren JF, Urrutia J, Huang J, Weinstein AS, Friedl V, Rettig M, Reiter RE, Spratt DE, Gleave M, Evans CP, Stuart JM, Chen Y, Feng FY, Small EJ, Witte ON, Xia Z, Transcriptional profiling identifies an androgen receptor activity-low, stemness program associated with enzalutamide resistance, Proc Natl Acad Sci U S A, 117 (2020) 12315–12323. [PubMed: 32424106]

[49]. Liang Y, Jeganathan S, Marastoni S, Sharp A, Figueiredo I, Marcellus R, Mawson A, Shalev Z, Pesic A, Sweet J, Guo H, Uehling D, Gurel B, Neeb A, He HH, Montgomery B, Koritzinsky M, Oakes S, de Bono JS, Gleave M, Zoubeidi A, Wouters BG, Joshua AM, Emergence of Enzalutamide Resistance in Prostate Cancer is Associated with BCL-2 and IKKB Dependencies, Clin Cancer Res, 27 (2021) 2340–2351. [PubMed: 33542074]

[50]. He Y, Wei T, Ye Z, Orme JJ, Lin D, Sheng H, Fazli L, Jeffrey Karnes R, Jimenez R, Wang L, Wang L, Gleave ME, Wang Y, Shi L, Huang H, A noncanonical AR addiction drives enzalutamide resistance in prostate cancer, Nat Commun, 12 (2021) 1521. [PubMed: 33750801]

[51]. Kim TH, Jeong JW, Song JH, Lee KR, Ahn S, Ahn SH, Kim S, Koo TS, Pharmacokinetics of enzalutamide, an anti-prostate cancer drug, in rats, Arch Pharm Res, 38 (2015) 2076–2082. [PubMed: 25956695]

[52]. Nam JS, Terabe M, Mamura M, Kang MJ, Chae H, Stuelten C, Kohn E, Tang B, Sabzevari H, Anver MR, Lawrence S, Danielpour D, Lonning S, Berzofsky JA, Wakefield LM, An anti-transforming growth factor beta antibody suppresses metastasis via cooperative effects on multiple cell compartments, Cancer Res, 68 (2008) 3835–3843. [PubMed: 18483268]

[53]. Park JI, Lee MG, Cho K, Park BJ, Chae KS, Byun DS, Ryu BK, Park YK, Chi SG, Transforming growth factor-beta1 activates interleukin-6 expression in prostate cancer cells through the

synergistic collaboration of the Smad2, p38-NF-kappaB, JNK, and Ras signaling pathways, Oncogene, 22 (2003) 4314–4332. [PubMed: 12853969]

[54]. Tovar Sepulveda VA, Falzon M, Parathyroid hormone-related protein enhances PC-3 prostate cancer cell growth via both autocrine/paracrine and intracrine pathways, Regul Pept, 105 (2002) 109–120. [PubMed: 11891011]

[55]. Guise TA, Yin JJ, Taylor SD, Kumagai Y, Dallas M, Boyce BF, Yoneda T, Mundy GR, Evidence for a causal role of parathyroid hormone-related protein in the pathogenesis of human breast cancer-mediated osteolysis, J Clin Invest, 98 (1996) 1544–1549. [PubMed: 8833902]

[56]. Santos R, Ursu O, Gaulton A, Bento AP, Donadi RS, Bologa CG, Karlsson A, Al-Lazikani B, Hersey A, Oprea TI, Overington JP, A comprehensive map of molecular drug targets, Nat Rev Drug Discov, 16 (2017) 19–34. [PubMed: 27910877]

[57]. Nadiminty N, Tummala R, Liu C, Yang J, Lou W, Evans CP, Gao AC, NF-kappaB2/p52 induces resistance to enzalutamide in prostate cancer: role of androgen receptor and its variants, Mol Cancer Ther, 12 (2013) 1629–1637. [PubMed: 23699654]

[58]. Kregel S, Chen JL, Tom W, Krishnan V, Kach J, Brechka H, Fessenden TB, Isikbay M, Paner GP, Szmulewitz RZ, Vander Griend DJ, Acquired resistance to the second-generation androgen receptor antagonist enzalutamide in castration-resistant prostate cancer, Oncotarget, 7 (2016) 26259–26274. [PubMed: 27036029]

[59]. Korpal M, Korn JM, Gao X, Rakiec DP, Ruddy DA, Doshi S, Yuan J, Kovats SG, Kim S, Cooke VG, Monahan JE, Stegmeier F, Roberts TM, Sellers WR, Zhou W, Zhu P, An F876L mutation in androgen receptor confers genetic and phenotypic resistance to MDV3100 (enzalutamide), Cancer Discov, 3 (2013) 1030–1043. [PubMed: 23842682]

Highlights

- Enzalutamide resistance is observed in PCa bone metastases.
- Enzalutamide-induced TGFBR2 decrease in osteoblasts contributes to drug resistance in PCa bone metastases.
- TGFBR2 decrease in osteoblasts is possibly through PTH1R-mediated endocytosis.
- Blocking PTH1R potentially overcomes enzalutamide resistance in PCa bone metastases.

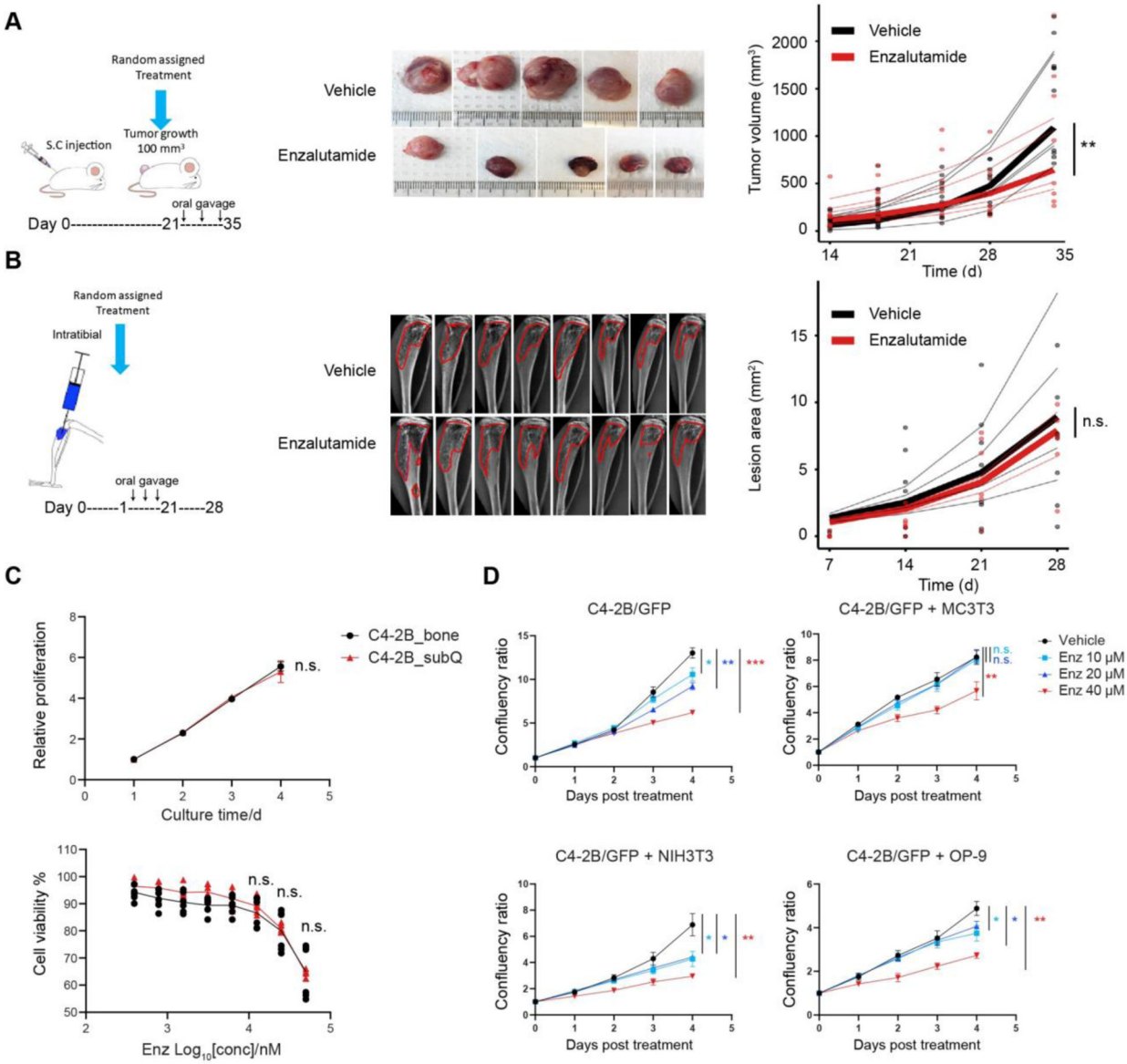

Figure 1. Enzalutamide resistance was observed in C4-2B-induced bone lesion development in mouse and C4-2B cells co-cultured with osteoblasts.

A, Enzalutamide inhibited subcutaneous C4-2B tumor growth. Left panel, the experimental design of subcutaneous xenografting, drug treatments, and analyses. Middle panel, the representative images of individual tumors harvested at the end time point. Right panel, tumor volume progression (n=9 for vehicle and n = 8 for enzalutamide). The bold lines are the mean values of the individual tumor volumes, shown in each thin line. $p = 0.001$ using a linear mixed-effect model. **B,** Enzalutamide treatment showed no effect on bone lesion development. Left panel, the experimental design of intratibial injections, drug treatments, and analyses. Middle panel, the representative images of individual bone lesions imaged at the end time point. Right panel, bone lesion development monitored weekly by X-ray. The bold lines are the mean values of the individual bone lesion areas, shown in each thin line. $p = 0.793$ using a linear mixed-effect model (n = 8 tibiae each). The experiments

in **A** and **B** were repeated and the same results were obtained. **C**, Cell proliferation and responsiveness to enzalutamide were not different between C4-2B cells sorted from the subcutaneous or intratibial tumors. Upper panel, the relative proliferation of live cells at the indicated dates normalized to the first day (n=3). Lower panel, the percentages of cell viability in enzalutamide treatment groups normalized to respective vehicle-treated groups (n=6). A two-tailed Wilcoxon rank-sum test followed by the Fisher's method was used to compare C4-2B_subQ and C4-2B_tibia, and no significant difference was observed, with $p = 0.691$ (upper) and $p = 0.108$ (lower). Cells were sorted from three individual mice. Experiments were repeated twice. **D**, Enzalutamide resistance was observed only in the co-culture of C4-2B cells with MC3T3-E1 cells. Relative confluency was determined as the GFP fluorescence area normalized to the confluent area observed at day 0. Results from three independent experiments (n=3) were plotted. The significance of difference in each enzalutamide-treated group compared to the corresponding vehicle-treated group at day 4 was evaluated by the Welch t-test.

For all panels, $*p < 0.05$, $**p < 0.01$, $***p < 0.001$, n.s.: non-significant.

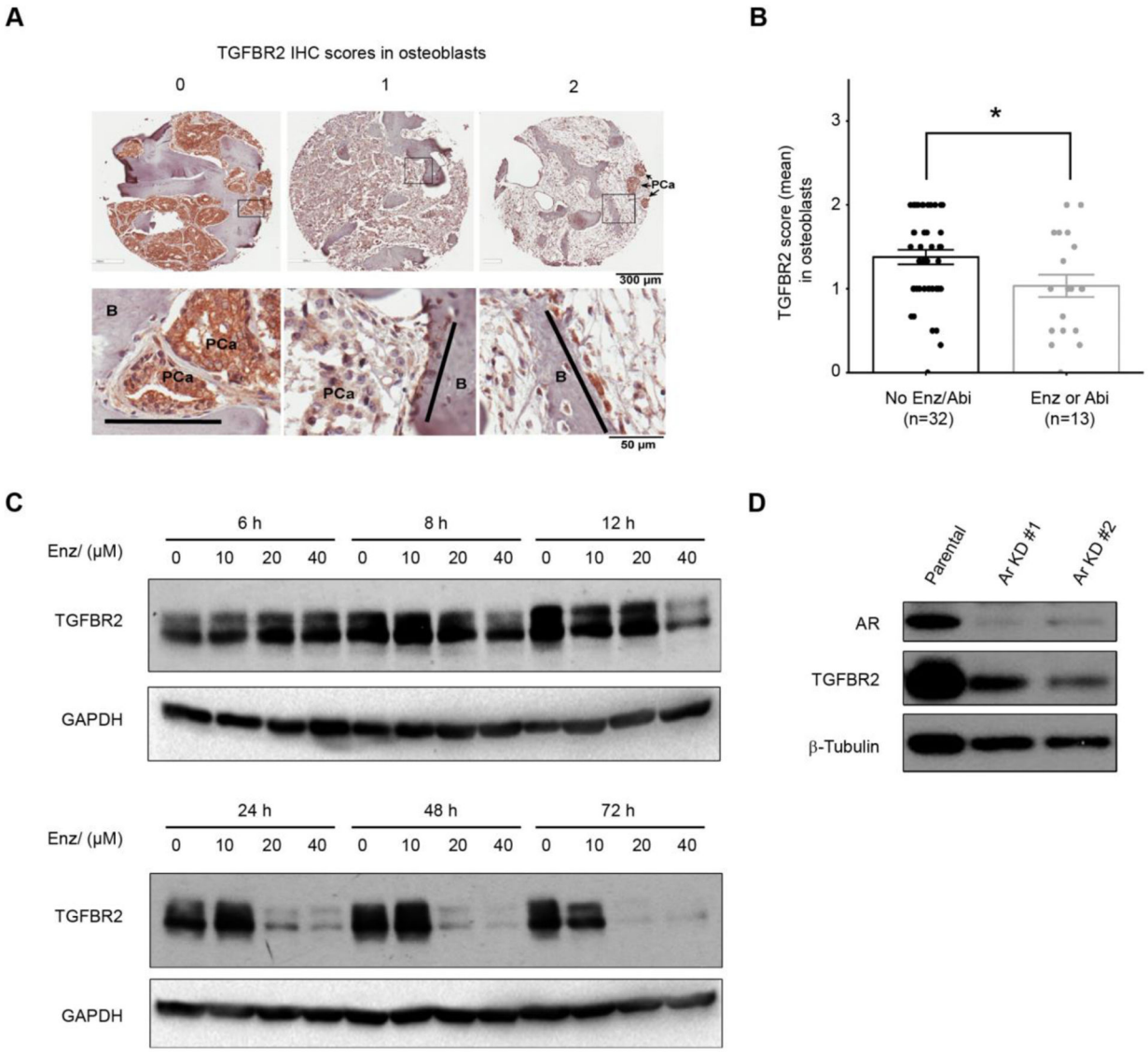

Figure 2. Enzalutamide decreased TGFBR2 levels in osteoblasts.

A, Representative immunohistochemistry (IHC) images of TGFBR2 in osteoblasts. Negative, moderate, and strong signal intensities were scored as 0, 1, and 2, respectively, in osteoblasts. Each sample was scored three times and then the average scores were used for analyses in **B**. Lines in zoomed lower panel highlight osteoblasts. PCa, prostate cancer cells; B, bone. Scale bar, upper panel 300 μm, lower panel 50 μm. **B**, Mean IHC scores for TGFBR2 expression in osteoblasts in different patient groups. Error bars indicate standard errors. Enz, enzalutamide. Abi, abiraterone. $p = 0.03$ using a linear mixed-effect model (n indicates patient number). *$p < 0.05$. **C**, Time- and dose-dependent effects of enzalutamide in MC3T3-E1 cells. 0 = vehicle (DMSO). **D**, TGFBR2 expression in *Ar*-knockdown osteoblasts. The *Ar* knockdown (KD) cells were generated using the CRISPR-Cas9 system. Parental, cells without guide RNA manipulation. *Ar* KD #1 and KD #2 were cells generated from two independent guide RNAs. All western blotting experiments were repeated three times.

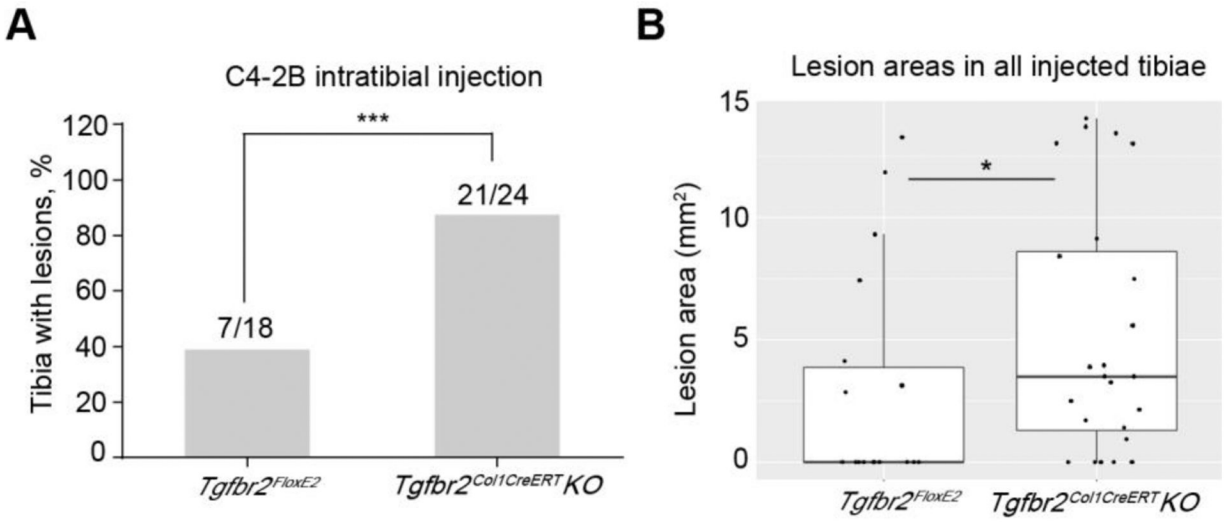

Figure 3. ***Tgfbr2*^{Col1CreERT} KO promoted C4-2B bone metastases.**

A, The proportion of tibiae with detectable C4-2B cell-induced bone lesions in all the injected tibiae was significantly higher ($p<0.001$, using a two-sample proportions test) in the *Tgfbr2*^{Col1CreERT} KO group relative to the *Tgfbr2*^{FloxE2} control group. The number of tibiae with detectable bone lesions identified by X-ray scanning of each group was counted 8 weeks after injection. **B,** Bone lesion areas in all the injected tibiae in the control *Tgfbr2*^{FloxE2} and *Tgfbr2*^{Col1CreERT} KO mice. Lesion area data collected at 5 weeks post-injection were plotted. $p = 0.0414$ using a Wilcoxon rank-sum test with continuity correction. For both panels, $*p<0.05$, $***p<0.001$.

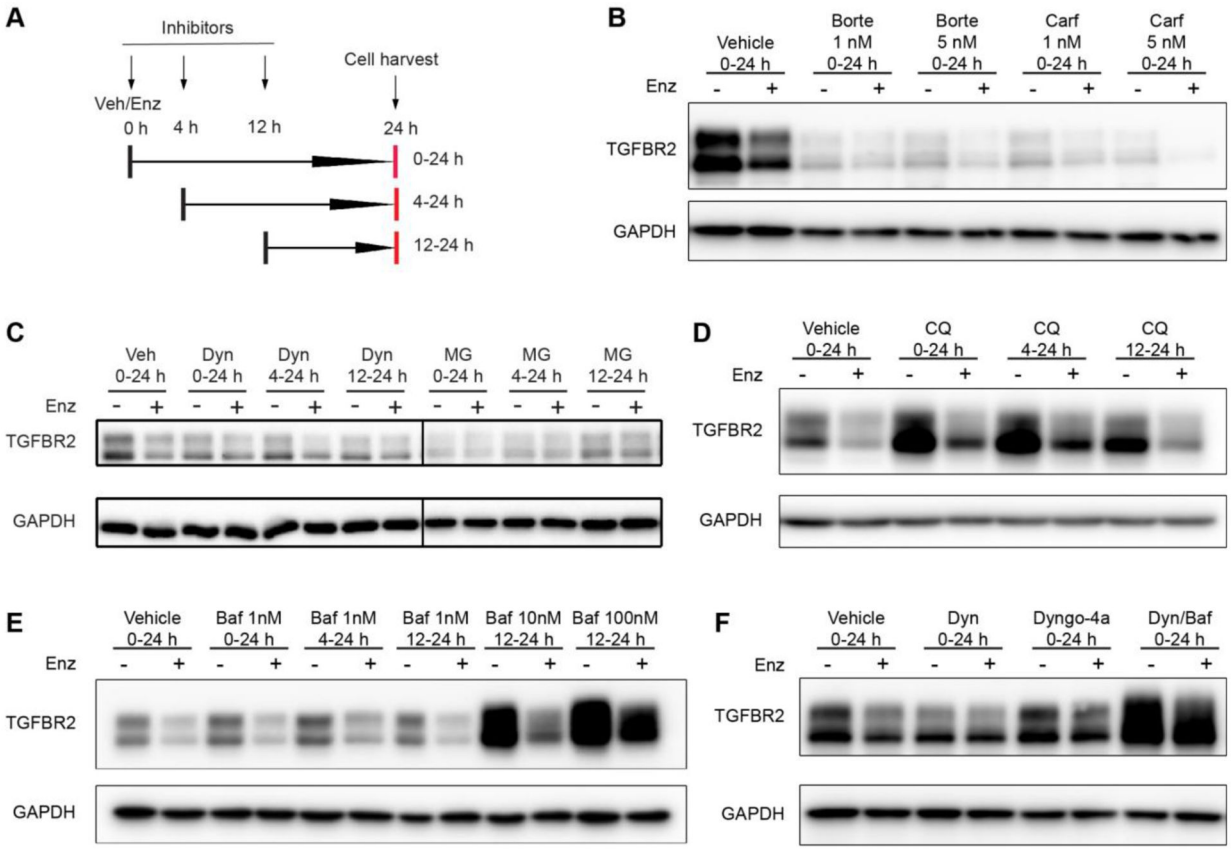

Figure 4. Enzalutamide-induced decrease in TGFBR2 level was possibly via endocytosis in MC3T3-E1 cells.

A, Schedule of drug treatments. MC3T3-E1 cells were treated with DMSO (−) or 40 μM enzalutamide (+) from 0 h to 24 h. Various inhibitors were introduced at 0 h, 4 h, or 12 h and cells were then harvested at 24 h. Total proteins were extracted from cells for western blotting. **B-F,** Representative western blots of MT3T3-E1 cells treated with: **B and C,** proteasome inhibitors bortezomib (Borte, 1 or 5 nM), carfilzomib (Carf, 1 or 5 nM), or MG132 (MG, 5 μM); **D and E**, autophagy/lysosome inhibitors chloroquine (CQ, 10 μM), bafilomycin A1 (Baf, 1, 10, or 100 nM); **C and F**, endocytosis inhibitors Dynasore (Dyn, 10 μM) or Dyngo-4a (10 μM) as well as Dyn plus Baf (10 nM). All the western blotting experiments were repeated three times.

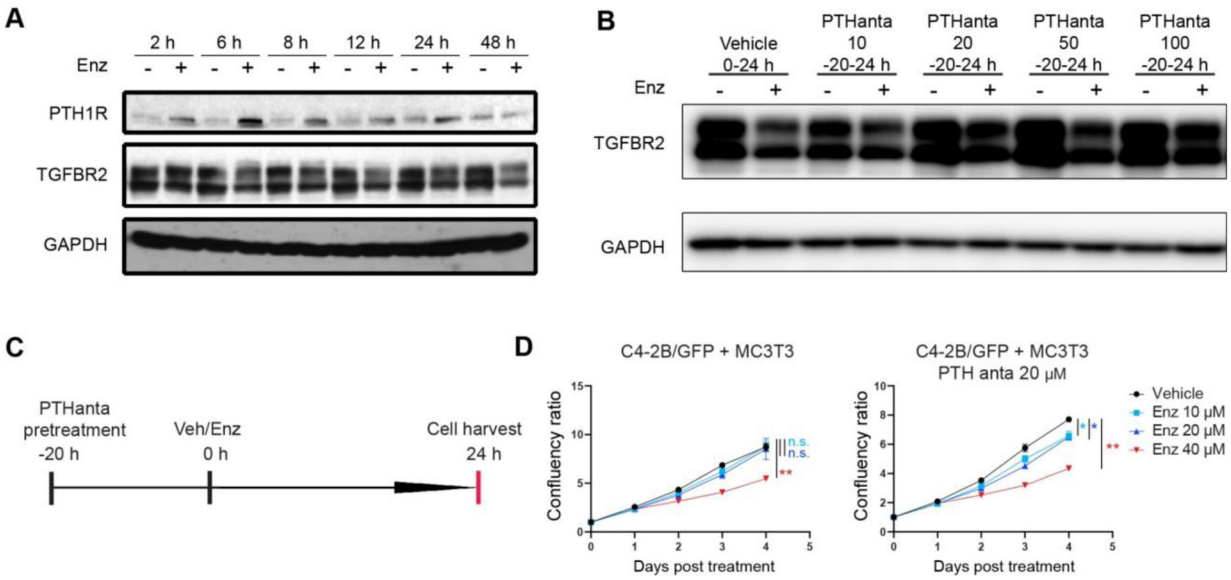

Figure 5. PTH1R mediated enzalutamide-induced decrease in TGFBR2 level in osteoblasts and enzalutamide resistance in co-culture of C4-2B and osteoblasts.

A, Enzalutamide increased PTH1R protein level before the decrease in TGFBR2 levels. MC3T3-E1 cells were treated with vehicle (−, DMSO) or enzalutamide (Enz, +, 40 μM). Total proteins were extracted from cells for western blotting. **B and C,** PTH1R antagonist rescued enzalutamide-decreased TGFBR2 in osteoblasts. MC3T3-E1 cells were pretreated with (Asn^{10}, Leu^{11}, D-Trp^{12}) PTHrP (7–34) amide (PTH1R antagonist, PTHanta, 10/20/50/100 ng/μL) for 20 h before the 24 h treatment of enzalutamide or vehicle (schedule shown in **C**). Total proteins were extracted from cells for western blotting (**B**). All the western blotting experiments were repeated three times. **D**, PTH1R antagonist restored enzalutamide response in the co-culture of C4-2B cells with MC3T3-E1 cells. Relative confluency was determined as the GFP fluorescence area normalized to the confluent area observed at day 0. Results from three independent experiments (n=3) were plotted. The significance of difference in each enzalutamide-treated group compared to corresponding vehicle-treated group at day 4 was evaluated by the Welch t-test. *p <0.05, **p<0.01, and n.s.: not significant.

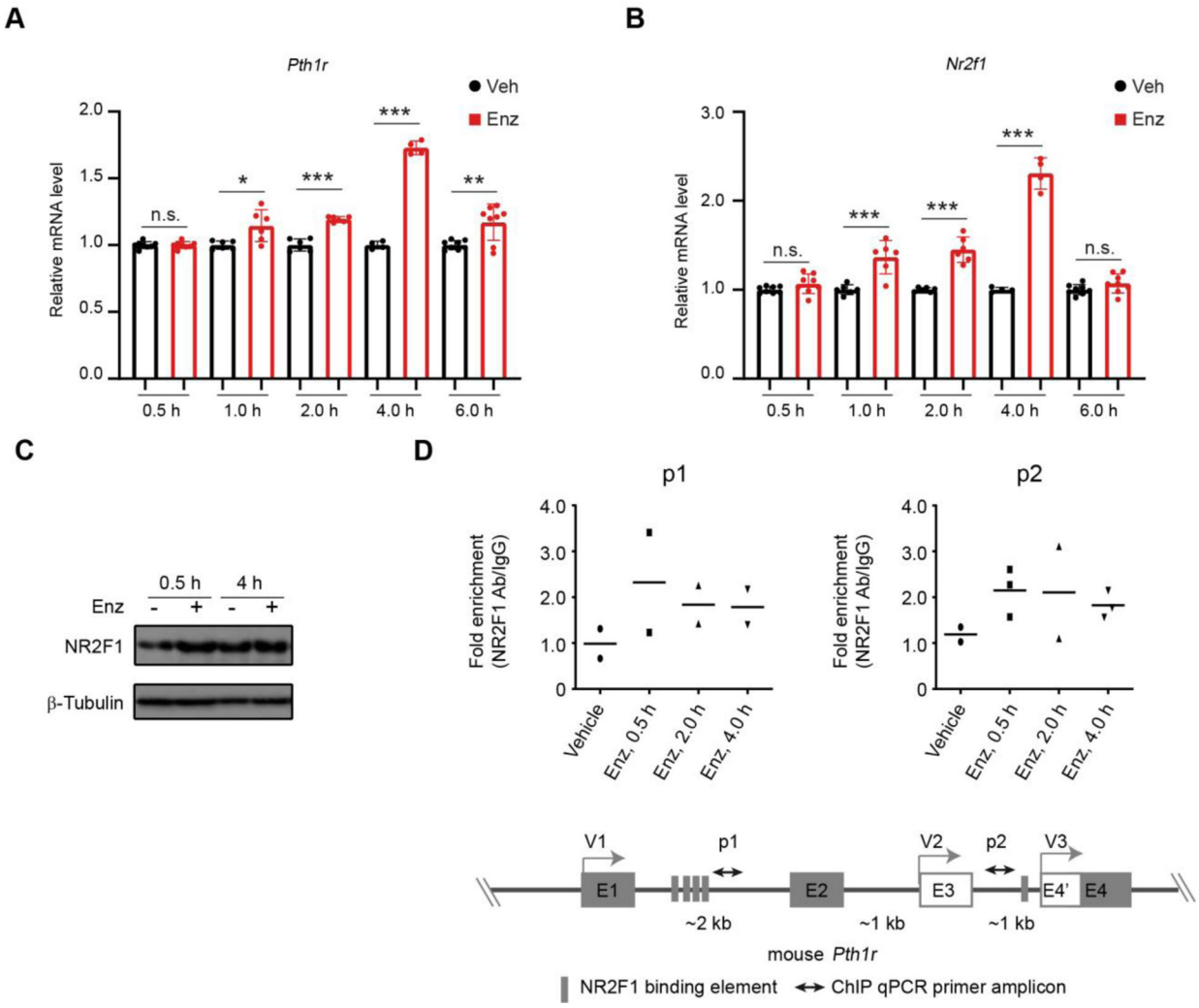

Figure 6. Enzalutamide induced NR2F1 expression and recruitment on *Pth1r* promoter.

A and B, Enzalutamide up-regulated the transcription of both *Pth1r* (**A**) and *Nr2f1* (**B**) in osteoblasts. MC3T3-E1 cells were treated with vehicle (DMSO) or enzalutamide (Enz, 40 μM) for the indicated time periods before being harvested for RNA extraction. *$p < 0.05$, **$p < 0.01$, ***$p < 0.001$ using the Welch t-test. **C,** Enzalutamide increased NR2F1 protein levels in osteoblasts. MC3T3-E1 cells were treated with vehicle (−, DMSO) or enzalutamide (Enz, +, 40 μM) for the indicated time periods before being harvested for immunoblotting. **D,** Enzalutamide increased the occupancy of NR2F1 at the *Pth1r* promoter in osteoblasts. NR2F1 binding elements appear frequently across the *Pth1r* promoter(s) of different *Pth1r* transcript variants (V1, V2, and V3). ChIP assay in MC3T3-E1 cells with different targeting primers (amplicons termed as p1 and p2) showed an increase in NR2F1 occupancy on *Pth1r* regulatory regions after enzalutamide treatment. Scatter plots display the mean and individual values from biological replicates. E1–E4 indicate the exons of different variants. Note that the *Pth1r* genomic region plotted here is not proportional to the actual length. All experiments were repeated three times.